J Incl Phenom Macrocycl Chem (2011) 69:91–99
DOI 10.1007/s10847-010-9818-0

ORIGINAL ARTICLE

Electrochemical and spectrophotometric determination of the formation constants of the ascorbic acid-β-cyclodextrin and dopamine-β-cyclodextrin inclusion complexes

M. Palomar-Pardavé · G. Alarcón-Ángeles · M. T. Ramírez-Silva · M. Romero-Romo · A. Rojas-Hernández · S. Corona-Avendaño

Received: 15 February 2010 / Accepted: 8 June 2010 / Published online: 30 June 2010

Abstract From UV–vis spectrophotometry and cyclic voltammetry it is demonstrated the interaction of dopamine, DA, and ascorbic acid, AA, with β-cyclodextrin, βCD, in aqueous media at pH 3.0. The formation constants of the respective inclusion complexes were also determined. The spectrophotometry data fed into the data processing software SQUAD, allowed calculation of the said constants for the AA–βCD complex (H_2AA–βCD) giving a value of 3236 M^{-1}, while for the dopamine complex DA–βCD (H_3DA+βCD) this was 5888 M^{-1}. From these results, the theoretical absorption spectra were generated which fitted quite well the experimental ones, thus indicating clearly that the constants are reliable. Moreover, from the cyclic voltammetry data, the stated constants were also calculated whereby that of the H_2AA–βCD gave a value of 3981 M^{-1} while for the dopamine complex DA–βCD (H_3DA+βCD) it was 4898 M^{-1}. It is noteworthy to say that these values were similar to those found through spectrophotometry.

Keywords Dopamine · Ascorbic acid · β-cyclodextrin · Inclusion complex · UV–vis spectrophotometry · Cyclic voltammetry

M. Palomar-Pardavé · G. Alarcón-Ángeles · M. Romero-Romo · S. Corona-Avendaño (✉)
Departamento de Materiales, Universidad Autónoma Metropolitana Azcapotzalco, Av. San Pablo #180, Col. Reynosa-Tamaulipas, C.P. 02200 México, DF, México
e-mail: sylvia_cav@yahoo.com.mx

M. T. Ramírez-Silva (✉) · A. Rojas-Hernández
Departamento de Química, Universidad Autónoma Metropolitana Iztapalapa, Av. San Rafael Atlixco #186, Col. Vicentina, C.P. 09340 México, DF, México
e-mail: mtrs218@xanum.uam.mx

Introduction

Cyclodextrins are crystalline compounds comprised of torus-like macro-rings of glucopyranose units, in particular the β-cyclodextrin, βCD, has seven glucose units. Various 3D structures result after joining the unit molecules that differ in their chemical and physical properties such as size, functionality or solubility, many of which are very interesting from a pharmaceutical point of view.

Derived from their peculiar molecular structure, these molecules display the chemical tendency to form inclusion complexes with other ionic species: these complexes are of great interest in practical applications and in fundamental research, because, when adequately manipulated, they provide information on non-covalent intermolecular forces. In this way, the βCD has been applied to develop chemical sensors for biologically interesting analytes, such as dopamine, DA, which is in its own right, an essentially important natural molecule, containing a catechol nucleus and an amine group on a chain with two-carbon atoms: *meta* or *para* to the phenolic hydroxyl groups, that are bioenergetic amines. Plainly said, dopamine plays a basic role as neurotransmitter in the central nervous system. Therefore, the DA is naturally expected to be used in diverse pharmaceuticals to treat some diseases [1]. However, its determination may be hindered by the presence of some interferents, of which the ascorbic acid, AA, exhibits an oxidation potential close to that of the DA, thus provoking an overlap of the voltammetric signals. Naturally, this has given rise to an increased interest to know the possible interactions between the complexes AA–βCD and DA–βCD.

Fukuda et al. [2], have reported that the α-amino acid 3,4-dihydroxyphenylalanine (DOPA) derivatives can be strongly included in the α-CD cavity. From this information, Fragoso

et al. [3], developed a novel strategy to detect DA in the presence of AA, at pH 7.0, that consists on the modification of gold electrodes with a mixed βCD and thioctic acid (TA) monolayer. The claim was that this provides the electrode with a molecular recognition motif (the CD) in addition to the electrostatic attraction of the TA. Moreover, Fragoso et al. [3] assumed, from literature data [3, 4], that CD forms stronger inclusion complexes with DA ($K_{DA} \sim 2000\ M^{-1}$ [2]) than with the AA ($K_{AA} = 130\ M^{-1}$ [4]), thus its presence in the monolayer in combination with TA increases the selectivity and sensitivity for the determination of the neurotransmitter by inducing a co-operative effect based on simultaneous electrostatic and host–guest interactions. However, even when this is clearly a good idea, the values of the apparent constant (K) that Fragoso et al. [3], mentioned are wrong since as one could see in the original references [2, 4] the apparent K_{AA} value is $2900 \pm 200\ M^{-1}$ at pH 6.9 [4] and K_{DA} for DA is not reported in reference [2].

On another respect, Gao et al. [5], reported the study of the inclusion complexes of catecholamines (dopamine and adrenaline) with βCD by cyclic voltammetry. The experimental results indicate that both catecholamines can form 1:1 inclusion complexes with βCD in aqueous solutions.

Therefore, the importance granted to knowing this sort of interactions, is the root cause for the objectives of this work, whereby, apart from calculating the acidity constants of the AA (K_a), we report also the complexation constants (K_f) between the DA–βCD and the AA–βCD, obtained through two different techniques, spectrophotometry UV–vis and cyclic voltammetry.

Experimental

Reagents and chemicals

All DA, AA, NaCl, HCl and β-CD solutions were prepared from Merck analytic grade reagents, where the HCl (37%) and H_3PO_4 acids were used to adjust the pH to 3.0. All solutions were prepared with deionised water Type I having 18.2 MΩ resistivity, free from organic matter obtained from a US Filter Pure-Lab Plus UV. Thus, the solutions prepared were deareated with nitrogen and freshly prepared prior to each determination. Also, they were protected from the incidence of light even during the performance of the experiments.

Instrumentation

The DA's and AA's electrochemical behaviour were characterized through cyclic voltammetry, CV. All determinations were carried out by means of a potentiostat-galvanostat Autolab PGSTAT 30. A carbon paste electrode, CPE, was prepared from graphite powder [6, 7] (Johnson Matthey 1 μm, 99.9%) and it was used as working electrode. A BAS MW-1032 Pt wire was used as counter electrode, and saturated Ag/AgCl was the reference also from BAS MF-2052, to which all potentials herein reported should be referred. The spectrophotometric behaviour was determined with the aid of a UV–vis Perkin Elmer Lambda 20 spectrophotometer.

Results and discussion

Determination of the AA's acidity constants

In order to understand and establish the complexation equilibria between the βCD, the DA and the AA at pH = 3, it is necessary to find out the acidity constants, pKa, of each species. In the DA's case these have calculated by means of UV–vis spectrophotometry and SQUAD, a computational software [8], which is fed with absorbance data and a chemical model that considers the possible chemical equilibria as basic input; this has already been reported by our group [9]. Therefore, the same method shall be used to calculate the AA's pKa. Figure 1 shows the absorption spectra of AA 0.1 mM at different pH. The spectral behaviour of the AA revealed two isosbestic points at 220 and 290 nm, which are associated to three acid–base species.

The spectral data obtained as a function of pH were used to assess the acidity constants by means of SQUAD [8]. The software was fed with 40 pH values within the 200–350 nm wavelength range (λ). The global formation constants calculated through this method are shown in Table 1.

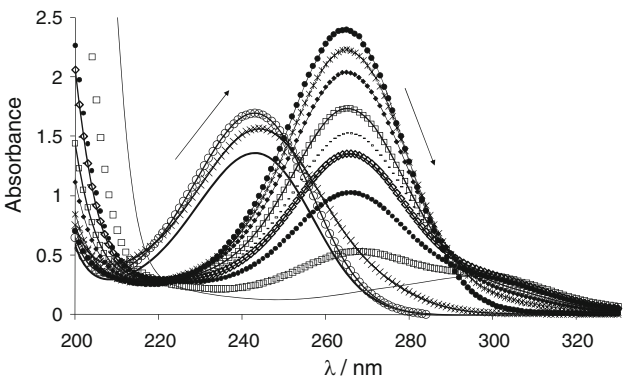

Fig. 1 Absorption spectral family of the AA 0.1 mM, for different pH values (—) 1.50, (⋇) 2.94, (⊖) 3.36, (●) 7.37, (⋇) 10.2, (◇) 10.76, (⊟) 10.98, (——) 11.14, (◇) 11.20, (●) 11.31, (□) 11.75, (_) 14.48

Table 1 Global formation constants of the AA evaluated by means of spectrophotometry, see Fig. 1 and SQUAD [8]

Equilibrium	log β
$H^+ + AA^{2-} \Leftrightarrow HAA^-$	11.36 ± 0.01
$2H^+ + AA^{2-} \Leftrightarrow H_2AA$	15.22 ± 0.02

The standard deviation for this data group was 9.42×10^{-2}

Determination of the inclusion constant of the AA with βCD

UV–vis spectrophotometry

From the values of the constants shown in Table 1 and following the methodology proposed by Rojas-Hernández et al. [10–13], a predominance zones diagram can be constructed, like that shown in Fig. 2, from which it becomes clear that at pH 3, AA is the neutral predominant species, termed H_2AA; therefore, the inclusion reaction of AA and βCD will be as indicated in Scheme 1 with a 1:1 interaction ratio.

To calculate the inclusion constant for Scheme 1, a spectrophotometry study of the neutral species H_2AA at different βCD concentrations and at constant pH = 3 was undertaken, the results of which are shown in Fig. 3a, where an absorption peak with its maximum at $\lambda = 242$ nm can be noted having also a small absorption increment as the βCD concentration increases in the system. This trend can be seen clearly in Fig. 3b, that plots the absorbance at this wavelength as a function of the βCD concentration in the system.

With the spectra reported in Fig. 3, the inclusion constant for Scheme 1 can be calculated using SQUAD [8], for which the most favourable equilibrium considered for the formation of the inclusion complex as discussed above for this pH, is the complex H_2AA–βCD. Table 2 shows the results obtained for the global formation constant, log β, and for formation, log K_f.

The molar absorptivity coefficients (ε) for the H_2AA y H_2AA–βCD species at each wave length (λ), calculated from the experimental spectra, see Fig. 3, and the SQUAD software are reported in Table 3. It is important to mention that βCD does not absorb in the wave length considered.

In order to gather evidence on the precision of the experimental values obtained through this method, a comparison of the experimental absorption spectra at different pβCD ($-\log[\beta\text{CD}]$) with the theoretical ones generated from the data refined of the formation constants and of the molar absorptivity coefficients, see below, was carried out.

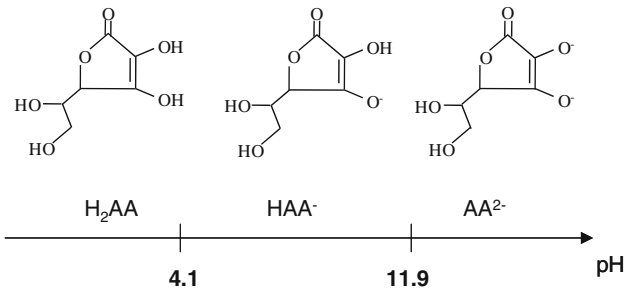

Fig. 2 Predominance zones diagram for the AA species and its structures as a function of pH

Theoretical absorption spectra

From the formation constants of the species, see Tables 1 and 2 and Eqs. 1 and 2 their respective molar fractions can be obtained

$$f_{\text{specie}} = \frac{1}{1 + 10^{(K_f - p\beta\text{CD})}} \quad (1)$$

$$f_{\text{complex}} = 10^{(K_f - p\beta\text{CD})}\left(\frac{1}{1 + 10^{K_f - p\beta\text{CD}}}\right) \quad (2)$$

Using the previous fractions and the overall concentration (C_t), the concentration of each species (C_{specie}) and (C_{complex}) is obtained from Eqs. 3 and 4.

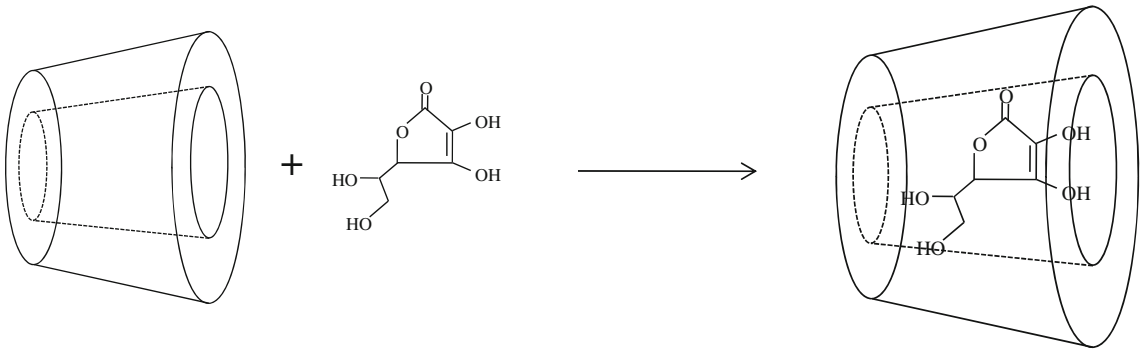

Scheme 1 Schematic reaction between the neutral AA species (H_2AA) and the βCD

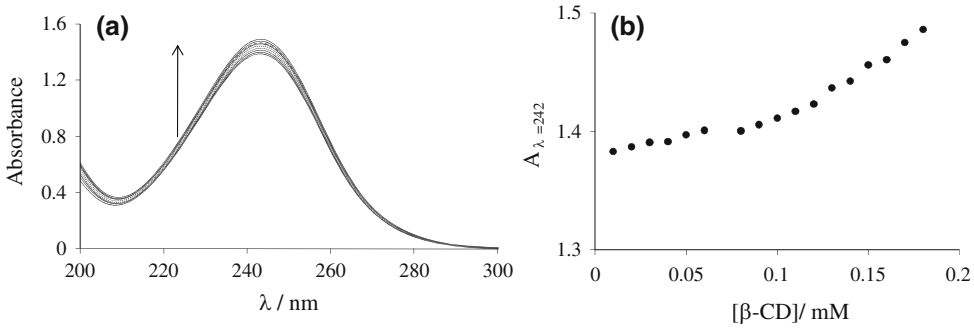

Fig. 3 **a** Spectral behaviour of AA 0.1 mM at pH 3 with different βCD concentrations. **b** Variation of the absorbance maximum at $\lambda = 242$ nm as a function of the βCD concentration

Table 2 Global formation constant of the complex H_2AA–βCD evaluated by means of experimental spectrophotometry data and SQUAD [8]

Equilibrium	
	log β
$2H^+ + AA^{2-} + \beta CD \Leftrightarrow H_2AA\beta CD$	18.73 ± 0.04
	log K_f
$H_2AA + \beta CD \Leftrightarrow H_2AA\beta CD$	3.51 ± 0.05

The standard deviation for this data group was 9.46×10^{-3}

$$C_{\text{specie}} = f_{\text{specie}}(C_t) \quad (3)$$

$$C_{\text{complex}} = f_{\text{complex}}(C_t) \quad (4)$$

From these concentrations and the molar absorptivity coefficients, see Table 3, the theoretical absorption at each wave length (λ) value, $A^{\lambda}_{\text{theoretical}}$, can be obtained using Eq. 5.

$$A^{\lambda}_{\text{theoretical}} = \varepsilon^{\lambda}_{\text{specie}}(C_{\text{speceie}}) + \varepsilon^{\lambda}_{\text{complex}}(C_{\text{complex}}) \quad (5)$$

Figure 4 shows the comparison of the theoretical absorption spectrum and that obtained experimentally, for pβCD = 3.7. Both spectra are indeed similar, which strongly suggests that the refining procedure of the calculated constant was appropriate.

With the respective K_f values and Eqs. 1 and 2 it is possible to construct the species distribution diagram shown in Fig. 5, for the complexes formed in aqueous solution as a function of pβCD.

Table 3 Molar absorptivity coefficients (ε) for the H_2AA and H_2AA–βCD species as a function of wave length (λ) calculated from the SQUAD software

λ/nm	$10^{-3}\ \varepsilon_{H_2AA}/M^{-1}cm^{-1}$	$10^{-3}\ \varepsilon_{H_2AA\beta_{CD}}/M^{-1}cm^{-1}$
200	3.39	6.82
204	2.50	4.77
208	2.16	3.67
212	2.37	3.55
216	3.00	4.17
220	3.93	5.25
224	5.08	6.57
228	6.36	8.02
232	7.68	9.54
236	8.85	10.95
240	9.63	11.98
244	9.81	12.37
248	9.28	11.92
252	8.11	10.74
256	6.51	9.06
260	4.81	7.20
264	3.30	5.48
268	2.16	4.05
272	1.38	2.94
276	0.87	2.06
280	0.55	1.34
284	0.34	0.81
288	0.21	0.41
292	0.12	0.16
296	0.07	0.00
300	0.03	0.00

Cyclic voltammetry

Cyclic voltammetry, CV, experiments were also recorded in the system CPE/0.1 M NaCl, 0.1 mM AA at pH 3 with different βCD concentrations to corroborate the calculated constant of the inclusion complex H_2AA–βCD estimated by means of UV–vis spectrophotometry. Figure 6a shows the CV's of the system CPE/0.1 M NaCl, 0.1 mM AA at pH 3 with different βCD concentrations, carried out, starting in the anodic direction; all cases depicted an oxidation peak, though when the potential was reversed there were no reduction peaks, which suggests that the AA exhibits an irreversible oxidation process. As the βCD concentration increases, this oxidation peak is shifted to greater potentials till at the βCD concentration 0.9 mM it remains constant; this trend can be more clearly appreciated in Fig. 6b.

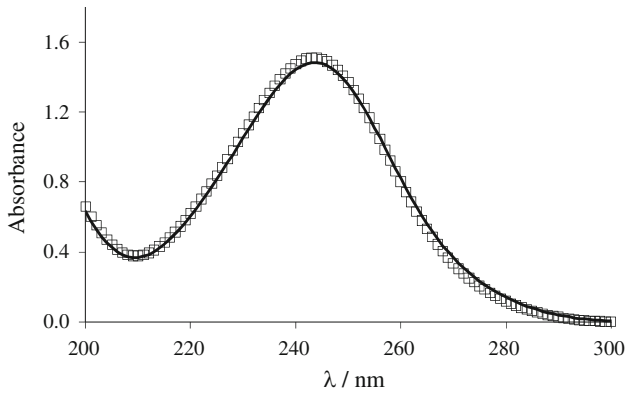

Fig. 4 Comparison of the theoretical (*Solid line*) spectrum generated using Eq. 5 and the date in Table 3 with the experimental absorption spectrum (*Open square*) obtained in the system: AA 0.1 mM at pH 3 with [βCD] = 0.2 mM, see Fig. 3a

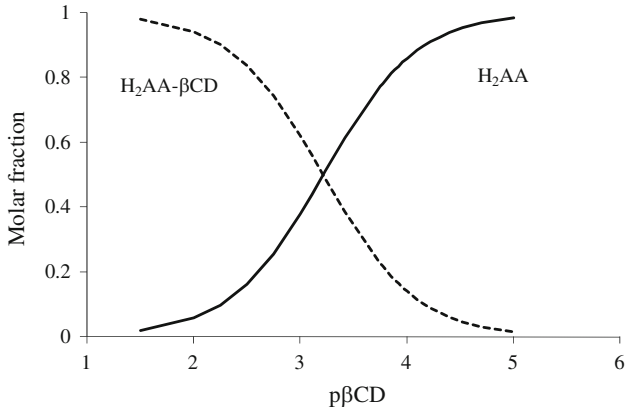

Fig. 5 Distribution diagram of the ascorbic acid species as a function of pβCD

With these data it becomes possible to calculate the inclusion constant using the method described by Gao et al. [5], using Eq. 6. The procedure was proposed earlier by

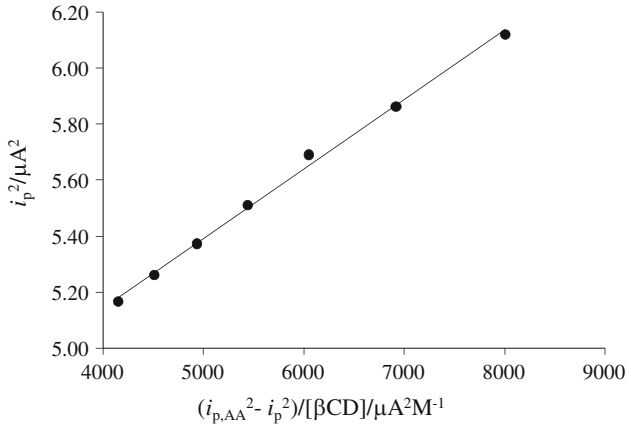

Fig. 7 Plot i_p^2 versus $i_{p(R)}^2 - i_p^2/[\beta CD]$, the current values were obtained from the voltammograms shown in Fig. 6a. The line was obtained from linear fitting of the experimental results

Evans and coworkers [14, 15] using diffusion coefficients instead of currents, and by Dang et al. [16] using currents

$$i_p^2 = \frac{K_d}{[\beta CD]}(i_{p(R)}^2 - i_p^2) + i_{p(R-\beta CD)}^2 \quad (6)$$

where i_p is the observed peak current; $i_{p(R)}$ and $i_{p(R-\beta CD)}$ are the peaks currents of the guest-free βCD and of the inclusion complex, respectively. Both $i_{p(R)}$ and $i_{p(R-\beta CD)}$ can be determined from the experiments. The inclusion dissociation constant, K_d, value can be obtained from the slope of the linear plot i_p^2 versus $i_{p(R)}^2 - i_p^2/[\beta CD]$ and from it the value of the inclusion formation constant, K_f, since $K_f = 1/K_d$.

Figure 7 shows the plot of i_p^2 versus $i_{p(R)}^2 - i_p^2/[\beta CD]$ where the equation of the straight line is given by $i_p^2/\mu A^2 = (0.0002478 \pm 0.0000062)\ M^{-1}\ (i_{p,DA}^2 - i_p^2/[\beta CD])/\mu A^2 M^{-1} + (4.152 \pm 0.036)\ \mu A^2$ with a correlation coefficient of 0.99. From the slope of the linear fit the following was obtained $K_d = 0.0002478 \pm 0.0000062$, which gives $pK_d = 3.60 \pm 0.03$; this value is very close to that found by means of UV–vis spectroscopy.

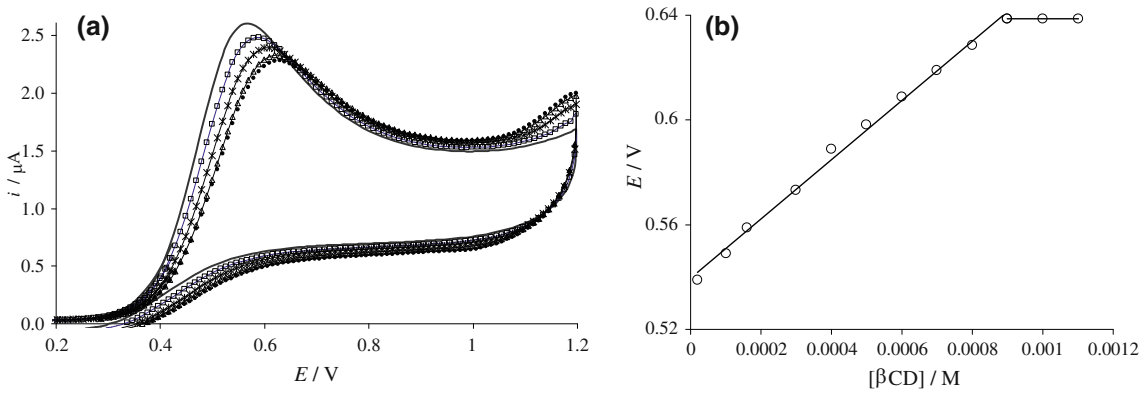

Fig. 6 **a** Cyclic voltammograms recorded in the system CPE/NaCl 0.1 M, AA 0.1 mM at pH 3 for different βCD additions (-) 0.2, (⊟) 0.4, (⨯) 0.6, (△) 0.8 and (●) 1 mM, at 100 mVs^{-1} scan rate. **b** Peak potential variations as a function of the βCD concentration

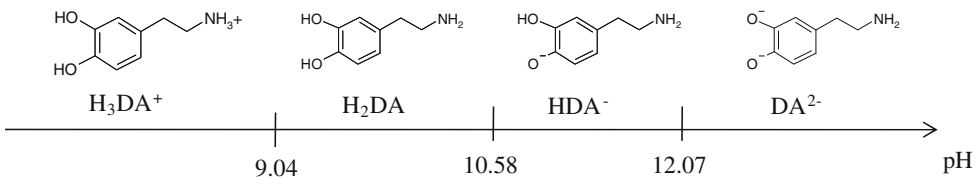

Fig. 8 Predominance zones diagram for the DA species and its structures as a function of pH

Determination of the DA–βCD inclusion constant

UV–vis spectroscopy

Following the same method as described above, and considering the predominance zones diagram shown in Fig. 8, proposed by Corona et al. [17], it can be established that the inclusion reaction between the DA and the βCD is as shown in Scheme 2, where the DA is fully protonated, H_3DA^+, as the solution's pH is 3.

The calculation of the formation constant of the inclusion complex H_3DA–βCD is made varying the βCD concentration in a DA 0.28 mM solution at pH 3 recording the UV–vis absorption spectrum for each βCD concentration. Figure 9 shows two absorption spectra obtained for the DA 0.28 mM and for the DA with βCD 2.5 mM. These spectra exhibit the DA characteristic band located at 279 nm that increased its absorbance as the βCD content increased in the system, see Fig. 9b. This increment can be associated with formation of the inclusion complex H_3DA–βCD. The absorbance change as a function of the molar relation between the [βCD]/[DA], showed that the stoichiometry of the complex H_3DA–βCD is 1:1.

With the data from the absorption spectra plotted as a function of the βCD concentration at pH 3 and from SQUAD [8], the reaction constants for Scheme 2 were calculated. The acidity constants of the DA were set considering the pKa reported by Sánchez-Rivera et al. [9]. A value of log $K_f = 3.77 \pm 0.16$ was refined by SQUAD as the complexation constant of the H_3DA–βCD inclusion complex. This value is greater than that found for the AA, thus the complex H_3DA–βCD is more stable than H_2AA–βCD.

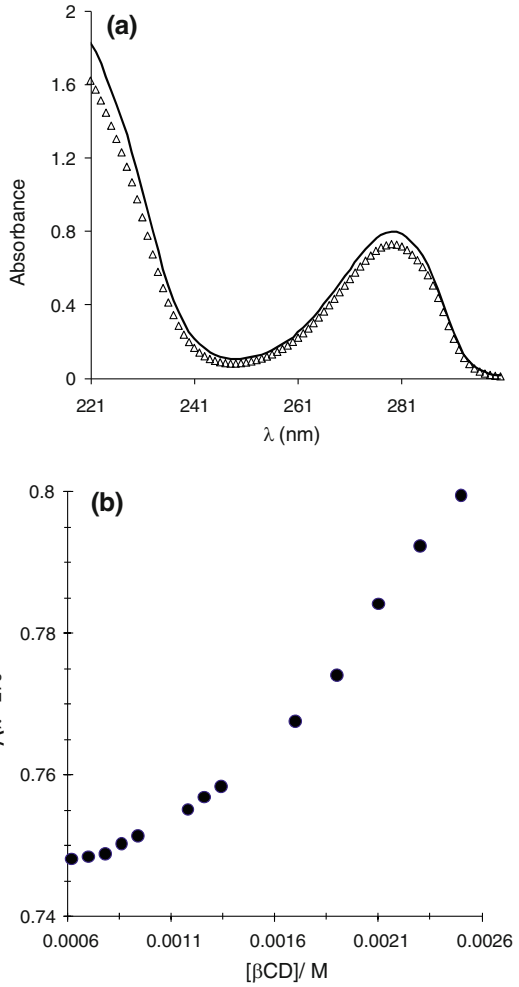

Fig. 9 **a** Spectral behaviour of the DA 0.28 mM (*open triangles*) and DA with βCD 2.5 mM (*solid line*) at pH 3. **b** Absorbance variation at $\lambda = 279$ nm as a function of the βCD concentration

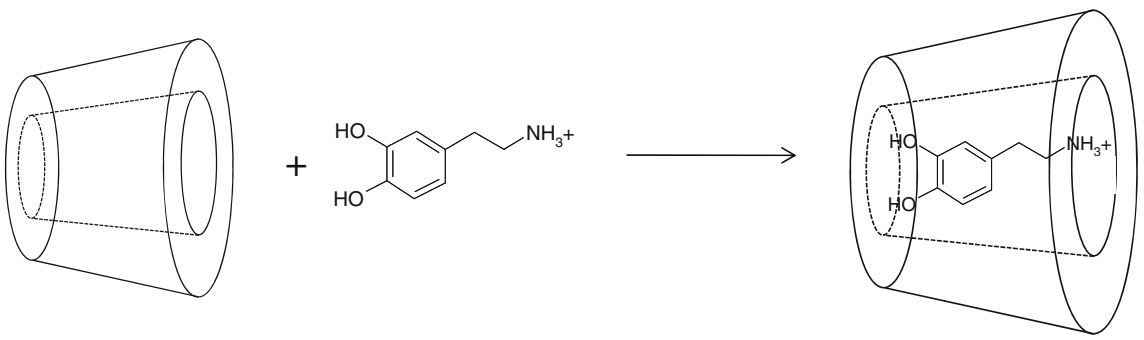

Scheme 2 Schematic reaction between the protonated species of the DA (H_3DA^+) and βCD

From the value of the H_3DA–βCD inclusion complex constant, the molar absorptivity coefficients reported in Table 4 and Eqs. 1–5, the theoretical spectrum of the system 0.28 M DA with βCD 0.9 mM was determined.

Figure 10 shows, as example, a comparison between spectra, the theoretical and the experimental one obtained at pβCD = 3. It becomes straightforward that the procedure is quite satisfactory for each and every wavelength considered, thus underlining the good quality of the fitting for all constants calculated by SQUAD [8].

With the respective K_f values and Eqs. 1 and 2, the distribution diagram shown in Fig. 11 was constructed.

Cyclic voltammetry

In order to carry out this study, βCD additions were made to a DA solution until the βCD concentration was 20 times greater than the DA concentration, to insure formation of the complex. The CV's from this study are shown in Fig. 12, at two βCD concentrations. The shift of anodic and cathodic peak's potential in the presence of βCD, is associated to formation of the inclusion complex, though it becomes evident that the said shift is greater for the cathodic peak.

Figure 13 shows the potential variation for the oxidation (a) and reduction (b) peaks, respectively, for both of which it becomes noticeable that oxidation and reduction are favored, overall making the process more reversible.

Table 4 Molar absorptivity coefficients (ε) for the H_3DA and $H_3DA\beta CD$ species as a function of wave length (λ) calculated from the SQUAD software

λ/nm	$10^{-3}\ \varepsilon_{H_3DA}/M^{-1}cm^{-1}$	$10^{-3}\ \varepsilon_{H_3DA\beta_{CD}}/M^{-1}cm^{-1}$
230	3.44	3.85
234	2.04	2.36
238	1.00	1.22
242	0.48	0.63
246	0.30	0.40
250	0.28	0.36
254	0.37	0.44
258	0.56	0.63
262	0.86	0.93
266	1.28	1.37
270	1.79	1.89
274	2.27	2.39
278	2.57	2.70
282	2.47	2.61
286	1.98	2.10
290	1.00	1.09
294	0.26	0.31
300	0.03	0.04

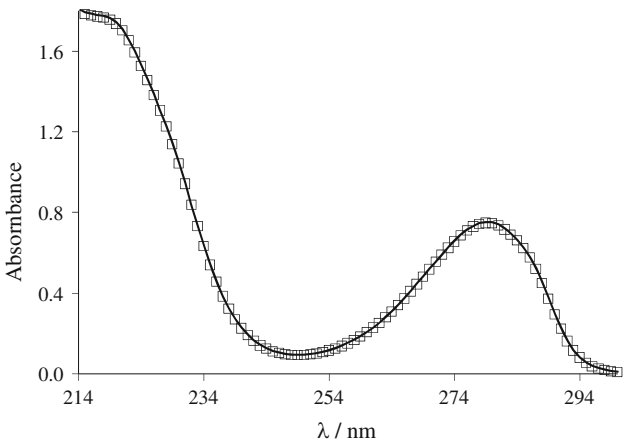

Fig. 10 Comparison of the theoretical (*solid line*) spectrum generated using Eq. 5 and the date in Table 4 with the experimental absorption spectrum (*open square*) obtained in the system: 0.28 M DA with [βCD] = 1 mM at pH 3

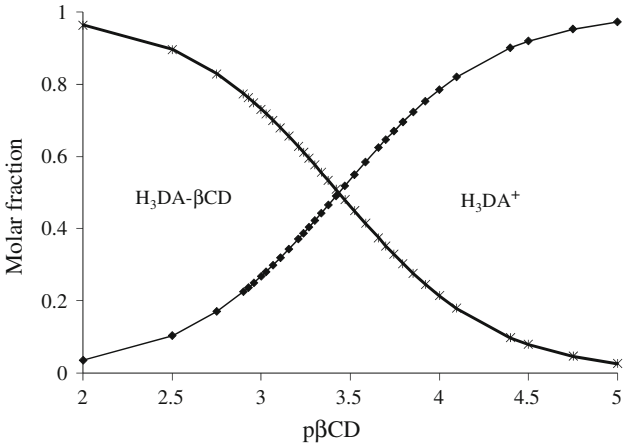

Fig. 11 Distribution diagram of the dopamine species as a function of pβCD

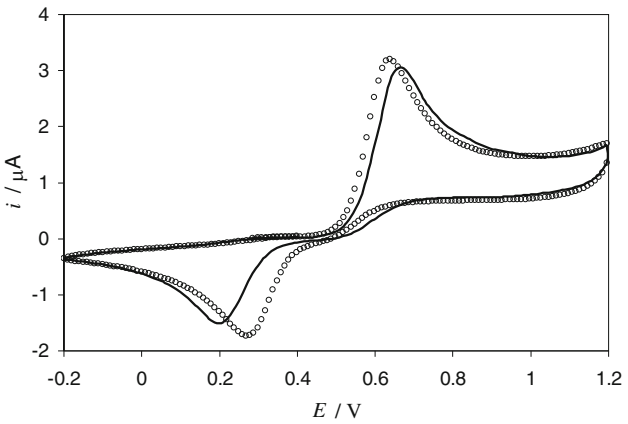

Fig. 12 Cyclic voltammograms recorded in the system CPE/NaCl 0.1 M, 0.1 DA mM at pH 3 for different βCD additions (*solid line*) 0 and (*open circle*) 0.2 mM, at 100 mVs^{-1} scan rate

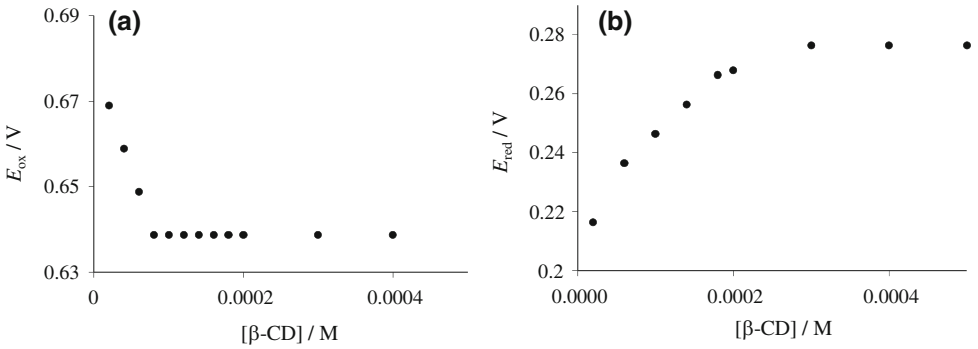

Fig. 13 Trends displayed by the peak potentials: **a** oxidation, E_{ox} and **b** reduction, E_{red}, obtained from the cyclic voltammograms shown in Fig. 12

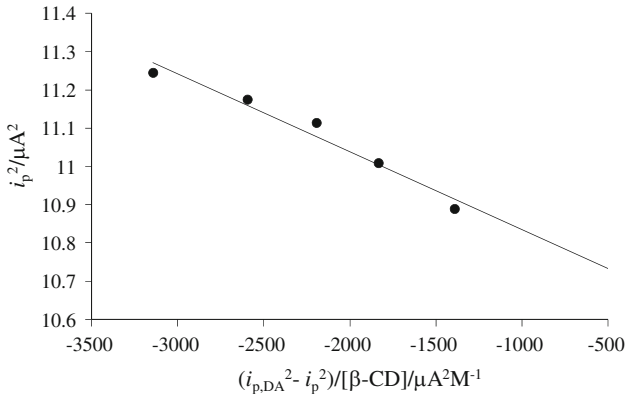

Fig. 14 Trend of the i_p^2 versus $(i_{p(R)}^2 - i_p^2)/[\beta CD]$ obtained from the data of the voltammograms shown in Fig. 12

In order to assess the complexation constant with these data, the method described above [5, 14–16], was followed; Fig. 14 shows the plot of i_p^2 versus $(i_{p(R)}^2 - i_p^2)/[\beta CD]$ where the expression for the resulting straight line is given by $i_p^2/\mu A^2 = -(0.00020 \pm 0.00003)\ M^{-1}\ (i_{p,DA}^2 - i_p^2/[\beta CD])/\mu A^2 M^{-1} + (10.6 \pm 0.09)\ \mu A^2$ with a correlation coefficient of 0.99. From the slope it results $K_d = 0.00020 \pm 0.00003$, from which one gets $pK_d = 3.70 \pm 0.15$; this value is quite close to that found by means of UV–vis spectroscopy.

Summarising, Table 5 shows the formation constants found from each of the methods used in this work for the complexes AA–βCD and DA–βCD. This sort of information can be useful for the development of diverse applications such as that reported by Chmurski et al. [18].

Table 5 Complexation constants formation evaluated by means of the different techniques employed in this work

Complex	Methodology	log K_f/M^{-1}
H_2AA–βCD	UV–vis spectrophotometry	3.51 ± 0.05
	Cyclic voltammetry	3.60 ± 0.03
H_3DA+βCD	UV–vis spectrophotometry	3.77 ± 0.16
	Cyclic voltammetry	3.70 ± 0.15

Conclusions

The formation of inclusion complexes between H_3DA–βCD and the H_2AA–βCD was demonstrated by spectrophotometry and electrochemical means, in aqueous media at pH 3. The values found through both methods were very similar, which emphasizes the reliability of the complexation constants derived. Further, the theoretical spectra represent the experimental behavior closely. The difference between the pK_f values shows that the H_2AA–βCD complex is more stable than the H_3DA–βCD. From the respective K_f values, distribution diagrams for these complexes were constructed as a fuction of pβCD.

Acknowledgments SCA 58250 and GAA 184930 express their gratitude to CONACyT for their postdoctoral and Ph.D., grants. MTRS thanks CONACyT for support through project 82932 and SCA for project 80305. Also GAA, SCA, MRR, MPP and MTRS gratefully thank the SNI for the distinction of their membership and the stipend received. MPP and MRR wish to thank the Departamento de Materiales, UAM-A, for the financial support given through projects (2261203, 2261204, 2261205).

References

1. Cui, H., Wu, L., Chen, J., Lin, X.: Multi-mode in situ spectro-electrochemical studies of redox pathways of adrenaline. J. Electroanal. Chem. **504**, 195–200 (2001)
2. Fukuda, T., Maeda, Y., Kitano, H.: Stereoselective inclusion of DOPA derivatives by a self-assembled monolayer of thiolated cyclodextrin on a gold electrode. Langmuir **15**, 1887–1890 (1999)
3. Fragoso, A., Almirall, E., Cao, R., Echegoyen, L., González-Jonte, R.: A supramolecular approach to the selective detection of dopamine in the presence of ascorbate. Chem. Commun. **19**, 2230–2231 (2004)
4. Manzanares, M.I., Solís, V., de Rossi, R.H.: Effect of cyclodextrins on the electrochemical behaviour of ascorbic acid on gold electrodes. J. Electroanal. Chem. **407**, 141–147 (1996)
5. Gao, Z.N., Wen, X.L., Li, H.L.: Study of the inclusion complexes of catecholamines with β-cyclodextrin by cyclic voltammetry polish. J. Chem. **76**, 1001–1007 (2002)
6. Ramírez-Silva, M.T., Palomar-Pardavé, M.E., González, I., Rojas-Hernández, A.: Carbon paste electrodes with electrolytic binder: influence of the preparation method. Electroanalysis **7**, 184–188 (1995)

7. Martínez, R., Ramírez-Silva, M.T., González, I.: Voltammetric characterization of carbon paste electrodes with a nonconducting binder. Part I: evidence of the influence of electroactive species dissolution into the paste on the voltammetric response. Electroanalysis **10**, 336–342 (1998)
8. Legget, D.: Computational methods for the determination of formation constants. Plenum press, New York (1995)
9. Sánchez-Rivera, A.E., Corona-Avendaño, S., Alarcón-Angeles, G., Rojas-Henández, A., Ramírez-Silva, M.T., Romero-Romo, M.A.: Spectrophotometric study on the stability of dopamine and the determination of its acidity constants. Spectrochim. Acta Part A **59**, 3193–3203 (2003)
10. Rojas-Henández, A., González, I.: Relationship of two-dimensional predominance-zone diagrams with conditional constants for complexation equilibria. Anal. Chim. Acta **187**, 279–285 (1986)
11. Rojas-Henández, A., Ramírez-Silva, M.T., Ibáñez, J.G., González, I.: Construction of multicomponent pourbaix diagrams using generalized species. J. Electrochem. Soc. **138**, 365–371 (1991)
12. Rojas-Hemández, A., Ramírez-Silva, M.T., González, I.: Equilibria among condensed phases and a multi-component solution using the concept of generalized species: Part I. Systems with mixed complexes. Anal. Chim. Acta **278**, 321–333 (1993)
13. Rojas-Hernández, A., Ramírez-Silva, M.T., González, I.: Equilibria among condensed phases and a multi-component solution using the concept of generalized species: part II. Systems with polynuclear species. Anal. Chim. Acta **278**, 335–347 (1993)
14. Matsue, T., Evans, D.H., Osa, T., Kobayashi, N.: Electron-transfer reactions associated with host-guest complexation. Oxidation of ferrocenecarboxylic acid in the presence of β-cyclodextrin. J. Am. Chem. Soc. **107**, 3411–3417 (1985)
15. Evans, D.H.: Two-component diffusion with reaction in chronoamperometry: approach to equilibrium conditions in the diffusion layer. J. Electroanal. Chem. **324**, 387–395 (1992)
16. Dang, X.-J., Tong, J., Li, H.-L.: The electrochemistry of the inclusion complex of anthraquinone with β-cyclodextrin studied by means of OSWV. J. Incl. Phenom. **24**, 275–286 (1996)
17. Corona-Avendaño, S., Alarcón-Ángeles, G., Rosquete-Pina, G.A., Rojas-Hernández, A., Gutiérrez, A., Ramírez-Silva, M.T., Romero-Romo, M., Palomar-Pardavé, M.: New insights on the nature of the chemical species involved during the process of dopamine deprotonation in aqueous solution: theoretical and experimental study. J. Phys. Chem. B **111**, 1640–1647 (2007)
18. Chmurski, K., Majewska, U.E., Bilewicz, R.: Analytical applications of gold electrodes modified with monolayers of thiolated cyclodextrins. J. Incl. Phenom. Macrocycl. Chem. **57**, 385–389 (2007)